

Sudden emergence of a shallow aragonite saturation horizon in the Southern Ocean

Gabriela Negrete-García^{1,6}, Nicole S. Lovenduski^{1*}, Claudine Hauri², Kristen M. Krumhardt^{3,7} and Siv K. Lauvset^{4,5}

Models project that with current CO₂ emission rates, the Southern Ocean surface will be undersaturated with respect to aragonite by the end of this century^{1–4}. This will result in widespread impacts on biogeochemistry and ocean ecosystems^{5–7}, particularly the health of aragonitic organisms, such as pteropods⁷, which can dominate polar surface water communities⁶. Here, we quantify the depth of the present-day Southern Ocean aragonite saturation horizon using hydrographic and ocean carbon chemistry observations, and use a large ensemble of simulations from the Community Earth System Model (CESM)^{8,9} to track its evolution. A new, shallow aragonite saturation horizon emerges in many Southern Ocean locations between now and the end of the century. While all ensemble members capture the emergence, internal climate variability may affect the year of emergence; thus, its detection may have been overlooked by ensemble average analysis in the past. The emergence of the new horizon is driven by the slow accumulation of anthropogenic CO₂ in the Southern Ocean thermocline, where the carbonate ion concentration exhibits a local minimum and approaches undersaturation. The new horizon is also apparent under an emission-stabilizing scenario indicating an inevitable, sudden decrease in the volume of suitable habitat for aragonitic organisms.

Rising atmospheric carbon dioxide (CO₂) levels resulting from the burning of fossil fuel and industrial and agricultural activities have been abated by CO₂ uptake by the ocean, which has absorbed nearly one-third of the total anthropogenic carbon added to the atmosphere^{10–12}. As the ocean absorbs atmospheric CO₂, its pH and carbonate ion concentration ($[CO_3^{2-}]$) decrease, thereby decreasing the saturation state ($\Omega = [Ca^{2+}][CO_3^{2-}]/K_{sp}$), which is the product of the concentrations of Ca²⁺ and CO₃²⁻, divided by the solubility product constant (K_{sp}) for calcium carbonate (CaCO₃) minerals, either aragonite (Ar) or calcite (Ca). Ω_{Ar} and Ω_{Ca} are defined as the ratio of the concentration of dissolved carbonate ions in a given solution to the concentration of dissolved ions in a saturated solution of aragonite and calcite, respectively. Aragonite and calcite are thermodynamically favoured to dissolve once Ω falls below the thermodynamic threshold $\Omega = 1$ and the depth at which this happens within the water column is referred to as the saturation horizon. Ocean acidification makes it harder for marine calcifying organisms (for example pteropods, corals, coccolithophores or foraminifera) to form and maintain their shells^{1,7,13}. While pteropods

exhibit a physiological negative response between $\Omega_{Ar} = 0.94$ and $\Omega_{Ar} = 1.12$ (ref. ⁷), soft clams, for example, are sensitive to a decrease in Ω_{Ar} well above this thermodynamic threshold¹⁴.

The Southern Ocean, defined as the region stretching from the Antarctic coastline to 40°S, is especially vulnerable to the effects of acidification relative to lower latitudes. Here, colder temperatures enhance the solubility of CO₂ and persistent upwelling brings carbon-rich water to the surface ocean^{13,15}. With current CO₂ emission rates, models project that the Southern Ocean's surface will be undersaturated with respect to aragonite by the end of the twenty-first century^{1,2,10}. This indicates that key marine calcifying organisms, such as those listed above, may not be able to cope well with future environmental conditions, which could change food web dynamics and have cascading effects on global ocean ecosystems^{3,13,15}. Ecosystem impacts in the Southern Ocean will serve as a bellwether for prospective impacts at mid and low latitudes where ocean acidification is projected to occur more slowly³.

Here, we use annual output from the CESM Large Ensemble (CESM-LE)^{8,9} to study the evolution of the aragonite saturation state under the high-emission Representative Concentration Pathway 8.5 (RCP8.5) (ref. ¹⁶) scenario (see Methods). The CESM is a state-of-the-art coupled climate model that simulates a unique climate trajectory in each ensemble member⁸. The large ensemble enables a robust estimate of the model's forced response to a given emission scenario and an evaluation of the spread in the response due to internal variability. We focus on the change in the saturation state of the CaCO₃ mineral aragonite, since it is more soluble than calcite at all temperatures and pressures in the ocean and will reach undersaturation earlier.

The depth of the present-day (defined throughout this work as year 2002) observed Southern Ocean aragonite saturation horizon exceeds 1,000 m across most of the basin. Within the core of the Antarctic Circumpolar Current (ACC), we find shallower saturation horizons (~400 m; Fig. 1a). The upwelling of deep water, which contains high CO₂ concentrations from remineralized organic matter, leads to elevated concentrations of dissolved inorganic carbon (DIC) and establishes a naturally shallow saturation horizon in the core of the ACC (refs. ^{17,18}). The deepest aragonite saturation horizon depths (~1,400 m) occur in the southwestern Indian Ocean, northeast of coastal Argentina and east of New Zealand.

CESM-LE exhibits a deeper present-day aragonite saturation horizon than that identified by the hydrographic and ocean carbon

¹Department of Atmospheric and Oceanic Sciences and Institute of Arctic and Alpine Research, University of Colorado Boulder, Boulder, CO, USA.

²International Arctic Research Center, University of Alaska Fairbanks, Fairbanks, AK, USA. ³Environmental Studies Program and Institute of Arctic and Alpine Research, University of Colorado Boulder, Boulder, CO, USA. ⁴NORCE Norwegian Research Centre, Bjerknes Centre for Climate Research, Bergen, Norway. ⁵Geophysical Institute, University of Bergen and Bjerknes Centre for Climate Research, Bergen, Norway. ⁶Present address: Integrative Oceanography Division, Scripps Institution of Oceanography, La Jolla, CA, USA. ⁷Present address: Climate and Global Dynamics Laboratory, National Center for Atmospheric Research, Boulder, CO, USA. *e-mail: nicole.lovenduski@colorado.edu

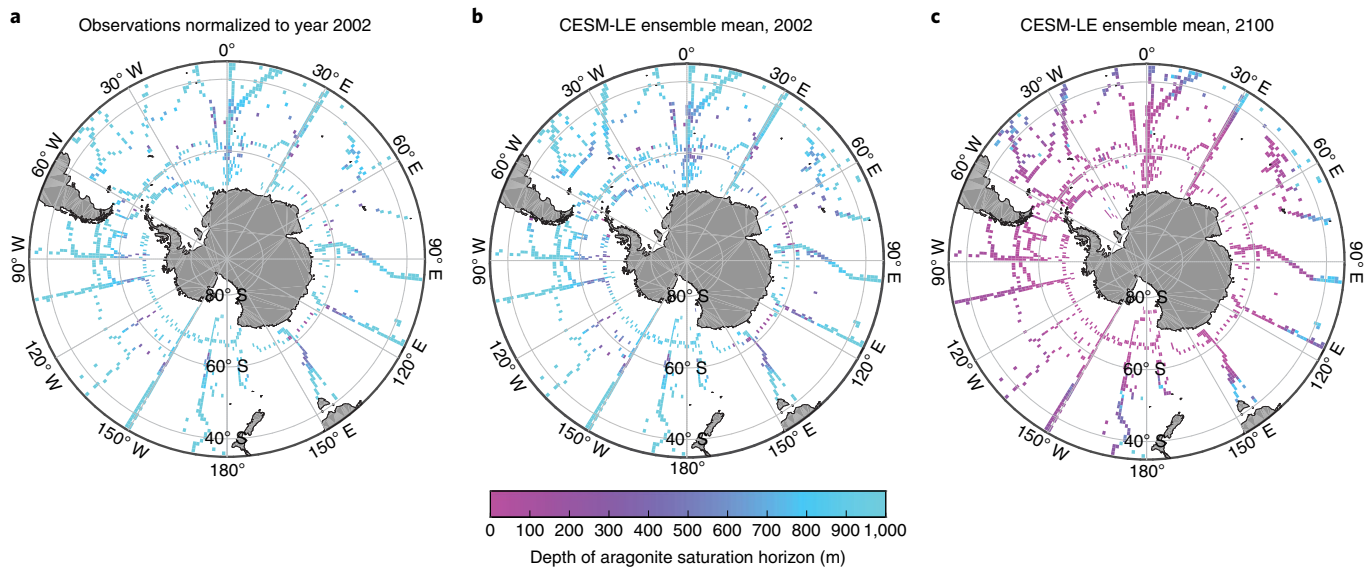


Fig. 1 | Depth of aragonite saturation horizon. a–c, Shows depth of the aragonite saturation horizon from GLODAPv2 bin-averaged DIC (normalized to year 2002) and alkalinity, as well as hydrography data from World Ocean Atlas (WOA 2009) sub-sampled at the GLODAPv2 data locations (a), CESM-LE in 2002, corrected for model bias using hydrographic observations (see Methods) (b), and CESM-LE in 2100 (c). Model projections are displayed in $1^\circ \times 1^\circ$ grid cells where there are sufficient GLODAPv2 data to identify a present-day saturation horizon.

chemistry observations^{19,20} (average bias 522 m; Supplementary Fig. 1). To correct for this bias, we use a procedure that pins the model projections to present-day observed distributions of carbonate chemistry, nutrients, temperature and salinity (see Methods). Hereafter, we refer to the bias-corrected model output. This bias correction procedure has been used in the past with much success¹¹. Moreover, it allows us to describe changes in the saturation horizon due to changes in DIC alone.

The CESM-LE ensemble mean depth of the aragonite saturation horizon, in the locations of the Southern Ocean (south 40°S) where present-day hydrographic data are available, is 83 m in 2100 (Fig. 1c), conforming to results of other recent studies^{1,2,10}. Annual average surface ocean aragonite undersaturation begins as early as 2006 in a few discrete locations. Aragonite undersaturation is projected across $\sim 20\%$ of the Southern Ocean surface by 2060, across $\sim 60\%$ of the surface by 2080 and $>80\%$ of the surface by 2100.

The CESM-LE projects the emergence of a new shallow saturation horizon across many locations in the Southern Ocean. This emergence is indicated by a step-change in saturation horizon depth of 400 m yr^{-1} or greater. In some locations, a step-change of as much as $1,000\text{ m}$ in a single year (Fig. 2) is projected. The depth and year of emergence varies spatially, reflecting both natural variation in the present-day saturation horizon depth and spatial variability in the physical circulation of the Southern Ocean. In the core of the ACC in the South Atlantic, we observe the largest step-changes in saturation horizon, ranging from 400 to $1,000\text{ m yr}^{-1}$ (Supplementary Fig. 2). The step-change is more moderate in the Indian sector, with the exception of a few points near the sea ice edge at 82.5°E . Step-changes of 500 m yr^{-1} or more are found throughout the Pacific Sector, extending into the subtropical latitudes. Step-changes also occur for a range of Ω_{Ar} thresholds (Supplementary Fig. 5).

The year of emergence of a shallow aragonite saturation horizon can vary across ensemble members, owing to their different representations of internal variability (Fig. 2, Supplementary Fig. 2), such as the El Niño Southern Oscillation and the Southern Annular Mode which can affect surface $[\text{CO}_3^{2-}]$ (refs. 21,22). For example, Fig. 2a illustrates that while all ensemble members project the emergence of a shallow saturation horizon at 0.5°E and 52.5°S , the year

of emergence occurs as early as 2006 in one ensemble member and as late as 2038 in another. This internally-driven spread in the year of emergence means that the average change in the saturation horizon (the mean across all ensemble members) is more moderate at this location. Similar conclusions can be drawn at other locations (Fig. 2b–e), suggesting that using the ensemble mean of several projections from one or more models (as is common practice in the Intergovernmental Panel on Climate Change reports and related publications) may misrepresent the emergence of a shallow horizon and the critical depth where this occurs.

The emergence of a shallow aragonite saturation horizon can be explained by the slow accumulation of anthropogenic carbon in the Southern Ocean thermocline that drives a local reduction of $[\text{CO}_3^{2-}]$ at the $[\text{CO}_3^{2-}]$ minimum (Fig. 3). The highest concentrations of $[\text{CO}_3^{2-}]$ are naturally found in the surface ocean and the lowest concentrations in the bottom of the water column, with a local minimum in the thermocline (Fig. 3c). This $[\text{CO}_3^{2-}]$ distribution reflects the imprint of surface photosynthesis and thermocline remineralization on the DIC concentration; photosynthesis draws down DIC and increases $[\text{CO}_3^{2-}]$, while remineralization produces DIC and decreases $[\text{CO}_3^{2-}]$ (ref. 23). In the Southern Ocean, the thermocline minimum in $[\text{CO}_3^{2-}]$ approaches the saturation concentration for mineral aragonite $[\text{CO}_3^{2-}]_{\text{sat(arag)}}$, which is primarily a function of pressure and increases with depth in the ocean²³ (Fig. 3c). Thus, an incremental addition of anthropogenic DIC to the thermocline has the potential to lower the $[\text{CO}_3^{2-}]$ below the critical $[\text{CO}_3^{2-}]_{\text{sat(arag)}}$ threshold, creating a sudden $\Omega=1$ horizon in the thermocline. This is illustrated at 0.5°E and 52.5°S , where a small increase in thermocline DIC from 2041 to 2042 causes a new saturation horizon to appear at a depth of 200 m (Fig. 3). Locations that fall within the region impacted by projected sea ice melt (for example, 32.5°E and -65.5°S , Fig. 2d) lack the carbonate ion minimum in the thermocline. Rapid undersaturation of surface waters here is driven by the invasion of anthropogenic DIC and/or by changes in the distribution of natural DIC as rapid ocean warming and freshening affects stratification and ventilation. Because of the technique we used to propagate the bias correction (see Methods),

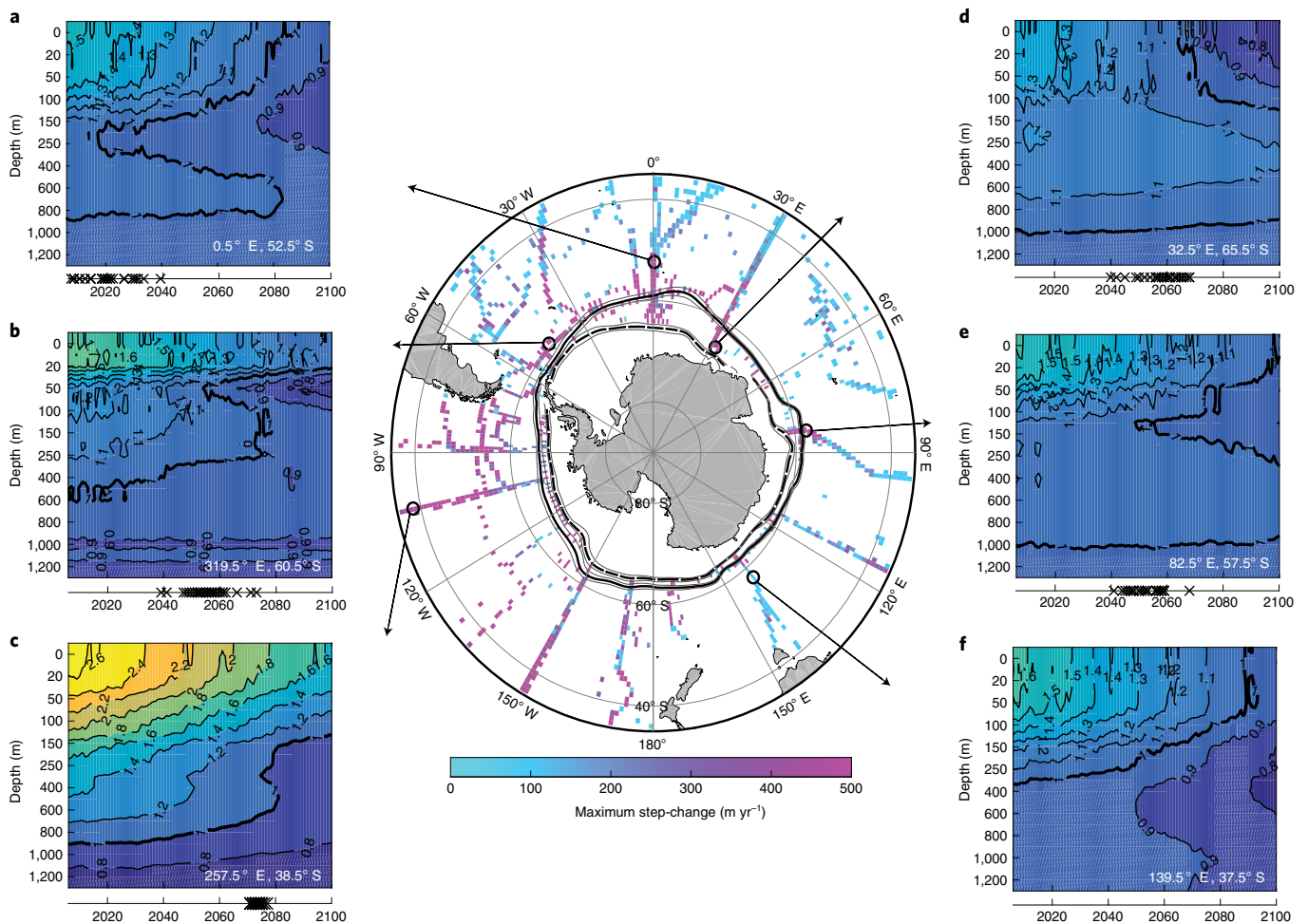


Fig. 2 | Emergence of shallow aragonite saturation horizon. Temporal evolution of upper water column aragonite saturation state in several locations, as projected by a single ensemble member of CESM-LE (RCP8.5): 0.5° E, 52.5° S (a), 319.5° E, 60.5° S (b), 257.5° E, 38.5° S (c), 32.5° E, 65.5° S (d), 82.5° E, 57.5° S (e) and 139.5° E, 37.5° S (f). Black X symbols on the time axis correspond to the year in which the new, shallow saturation horizon emerges in individual ensemble members. The centre map shows the maximum step-change in aragonite saturation horizon from a single CESM-LE ensemble member over the period 2006–2100 at each location in the Southern Ocean (m yr^{-1}). The black solid (dashed) line shows the average sea ice extent in 2006 (2100) and thin grey lines show one standard deviation sea ice extent across the CESM-LE ensemble members. Model projections are displayed in $1^\circ \times 1^\circ$ grid cells where there are sufficient GLODAPv2 data to identify a present-day saturation horizon.

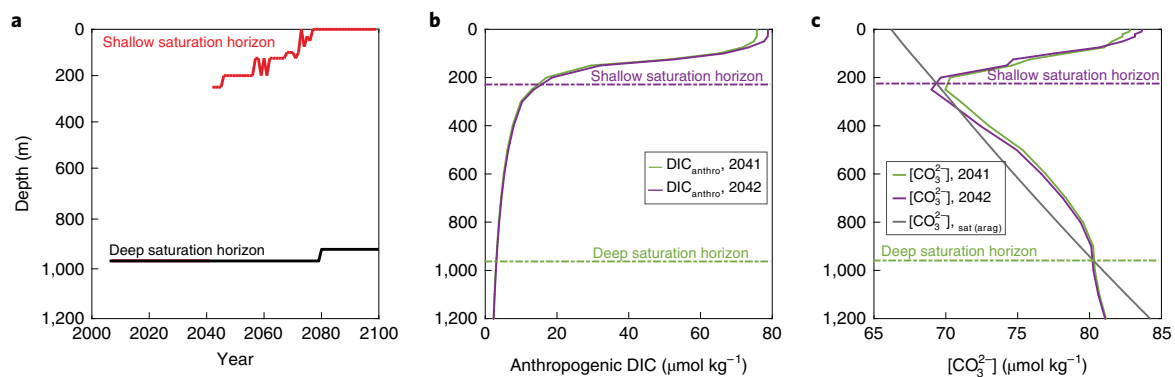


Fig. 3 | Drivers of the sudden emergence of the shallow horizon. a, Temporal evolution of the depth of the aragonite saturation horizon at 0.5° E and 53.5° S from a single CESM-LE ensemble member. b, c, Vertical profiles of anthropogenic DIC concentration ($\mu\text{mol kg}^{-1}$) and the corresponding depth of the aragonite saturation horizon (b), and carbonate ion concentration ($\mu\text{mol kg}^{-1}$) from the same location and ensemble member before and after the step-change in aragonite saturation horizon (2041 and 2042, respectively) (c).

internal variability and externally-forced changes in temperature, salinity, alkalinity and nutrients have no direct consequences on the depth of the horizon. However, internally- and externally-driven

changes in ocean circulation can affect the interior ocean distribution of DIC and thus indirectly impact the depth of the aragonite saturation horizon.

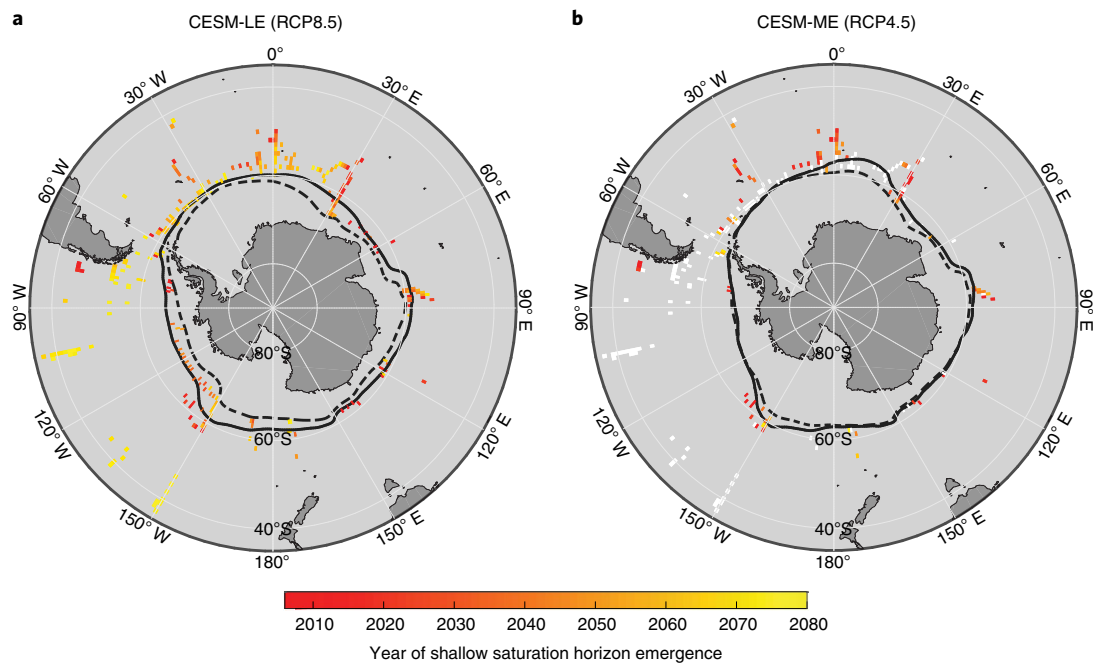


Fig. 4 | Year of emergence of shallow saturation horizon. **a,b**, Projected year of emergence of new, shallow saturation horizons from a single ensemble member under RCP8.5 (**a**) and RCP4.5 (**b**) emission scenarios over 2006–2080. The emergence of a shallow saturation horizon is defined as the first year where a step-change in saturation horizon greater than 500 m yr^{-1} occurs. Locations where the emergence of shallow horizons occur under the high-emission scenario but not the stabilizing-emission scenario are shaded white in **b**. Black solid (dashed) line shows the average sea ice extent in 2006 (2080).

An ensemble of CESM simulations run under the stabilizing-emission scenario RCP4.5 indicates that the emergence of a shallow saturation horizon is unavoidable across a large swath of the Southern Ocean, although the year of emergence can be delayed substantially (Fig. 4). This medium ensemble (CESM-ME, so-called because it has nine ensemble members, see Methods) simulates a similar range of internal variability in the depth of the saturation horizon but with a slower increase in anthropogenic DIC in the Southern Ocean thermocline than that of CESM-LE (RCP8.5). The emergence of a shallow aragonite saturation horizon (defined as the first year where a step-change of saturation horizon is greater than 500 m yr^{-1}) occurs approximately 20 years later in CESM-ME (RCP4.5) compared to CESM-LE (RCP8.5). Nevertheless, increases in thermocline DIC occur throughout the southern-most South Atlantic and Indian basins, causing the emergence of a shallow horizon in all CESM-ME (RCP4.5) ensemble members (Supplementary Fig. 3). Across the subtropical South Pacific, where the emergence of shallow saturation horizons were projected in all of the CESM-LE (RCP8.5) ensemble members by 2080 (Supplementary Fig. 2), the CESM-ME (RCP4.5) shows no emergence of a shallow horizon (Supplementary Fig. 3), probably because it occurs later than 2080 (which is the end-date for CESM-ME simulations).

Our analysis implies that Southern Ocean acidification-sensitive organisms will experience a sudden decrease in the volume of their suitable habitat, including shelled pteropods^{1,5–7}, foraminifers, cold-water corals^{3,24}, sea urchins, molluscs³ and coralline algae^{1,3,24}. Shelled pteropods, the major planktonic producers of aragonite, might be especially vulnerable to these changing conditions since they typically live in the upper 300 m and form an integral component of polar and subpolar food webs^{5–7}. Pteropods account for a large portion of the flux of CaCO_3 to the deep ocean in the Southern Ocean^{25,26} and therefore a decrease in pteropod populations would decrease the amount of CaCO_3 (and, thus, alkalinity) exported to

depth. Increased alkalinity remaining in the upper ocean could allow increased oceanic absorption of atmospheric CO_2 , an important negative feedback on climate change. Due to the rapid progression of ocean acidification, pteropods may have a limited time to adapt to a corrosive environment since they produce only two generations per year²⁷. While the emergence of a shallow saturation horizon has been projected in coastal upwelling systems²⁸, the Southern Ocean is characterized by much lower natural variability in surface ocean $[\text{CO}_3^{2-}]$ (refs. ^{21,29}). Given this low background variability, organisms in the Southern Ocean may not be able to contend with sudden changes in the volume of their habitat, with far-reaching consequences for fisheries, economies, and livelihoods.

Due to the lack of ship-board wintertime observations, the CESM aragonite saturation horizon is unable to be verified during winter months. Therefore, this analysis focuses only on the annual mean values of aragonite saturation state in the Southern Ocean. Other studies^{4,30}, however, show an intense surface wintertime minimum in CO_3^{2-} south of the Antarctic Polar Front, which, combined with increasing amounts of anthropogenic CO_2 , will probably lead to earlier undersaturation events during winter. Finally, we note that while CESM-LE and CESM-ME do not represent the potential physiological responses of organisms to ocean acidification, such as altered calcification rates, N_2 fixation, and net primary production, these may also cause future changes in local carbonate chemistry with potentially important climate-carbon feedbacks¹⁵.

Online content

Any methods, additional references, Nature Research reporting summaries, source data, statements of data availability and associated accession codes are available at <https://doi.org/10.1038/s41558-019-0418-8>.

Received: 29 July 2018; Accepted: 22 January 2019;
Published online: 11 March 2019

References

- Orr, J. C. et al. Anthropogenic ocean acidification over the twenty-first century and its impact on calcifying organisms. *Nature* **437**, 681–686 (2005).
- Hauri, C., Friedrich, T. & Timmermann, A. Abrupt onset and prolongation of aragonite undersaturation events in the Southern Ocean. *Nat. Clim. Change* **6**, 172–176 (2016).
- Fabry, V. J., McClintock, J. B., Mathis, J. T. & Grebmeier, J. M. Ocean acidification at high latitudes: the bellwether. *Oceanography* **22**, 160–171 (2009).
- McNeil, B. I. & Matear, R. J. Southern Ocean acidification: a tipping point at 450-ppm atmospheric CO₂. *Proc. Natl Acad. Sci. USA* **105**, 18860–18864 (2008).
- Moy, A. D., Howard, W. R., Bray, S. G. & Trull, T. W. Reduced calcification in modern Southern Ocean planktonic foraminifera. *Nat. Geosci.* **2**, 276–280 (2009).
- Hunt, B. et al. Pteropods in Southern Ocean ecosystems. *Prog. Oceanogr.* **78**, 193–221 (2008).
- Bednarek, N. et al. Extensive dissolution of live pteropods in the Southern Ocean. *Nat. Geosci.* **5**, 881–885 (2012).
- Kay, J. E. et al. The Community Earth System Model (CESM) Large Ensemble project: A community resource for studying climate change in the presence of internal climate variability. *Bull. Am. Meteorol. Soc.* **96**, 1333–1349 (2015).
- Lovenduski, N. S., McKinley, G. A., Fay, A. R., Lindsey, K. & Long, M. C. Partitioning uncertainty in ocean carbon uptake projections: Internal variability, emission scenario, and model structure. *Global Biogeochem. Cycles* **30**, 1276–1287 (2016).
- Feely, R. A. et al. Impact of anthropogenic CO₂ on the CaCO₃ system in the oceans. *Science* **305**, 362–366 (2004).
- Ciais, P. et al. in *Climate Change 2013: The Physical Science Basis* (eds Stocker, T. F. et al.) Ch. 6 (IPCC, Cambridge Univ. Press, 2013).
- Le Quere, C. et al. Global carbon budget 2017. *Earth Syst. Sci. Data* **10**, 405–448 (2018).
- Kroeker, K. J. et al. Impacts of ocean acidification on marine organisms: quantifying sensitivities and interaction with warming. *Global Change Biol.* **19**, 1884–1896 (2013).
- Ries, J. B., Cohen, A. L. & McCorkle, D. C. Marine calcifiers exhibit mixed responses to CO₂-induced ocean acidification. *Geology* **37**, 1131–1134 (2009).
- Doney, S. C., Fabry, V. J., Feely, R. A. & Kleypas, J. A. Ocean acidification: the other CO₂ problem. *Annu. Rev. Marine Sci.* **1**, 169–192 (2009).
- Sanderson, B. M., Oleson, K. W., Strand, W. G., Lehner, F. & O'Neill, B. C. A new ensemble of GCM simulations to assess avoided impacts in a climate mitigation scenario. *Clim. Change* **146**, 303–318 (2015).
- Lovenduski, N. S., Gruber, N. & Doney, S. C. Toward a mechanistic understanding of the decadal trends in the Southern Ocean carbon sink. *Global Biogeochem. Cycles* **22**, GB3016 (2008).
- Marshall, J. & Speer, K. Closure of the meridional overturning circulation through Southern Ocean upwelling. *Nat. Geosci.* **5**, 171–180 (2012).
- Olsen, A. et al. The Global Ocean Data Analysis Project version 2 (GLODAPv2)—an internally consistent data product for the world ocean. *Earth Syst. Sci. Data* **8**, 297–323 (2016).
- Lauvset, S. K. et al. A new global interior ocean mapped climatology: the 1°×1° GLODAP version 2. *Earth Syst. Sci. Data* **8**, 325–340 (2016).
- Conrad, C. J. & Lovenduski, N. S. Climate-driven variability in the Southern Ocean carbonate system. *J. Clim.* **28**, 5335–5350 (2015).
- Xue, L. et al. Climatic modulation of surface acidification rates through summertime wind forcing in the southern ocean. *Nat. Commun.* **9**, 3240 (2018).
- Sarmiento, J. L. & Gruber, N. *Ocean Biogeochemical Dynamics* (Princeton Univ. Press, Princeton, 2006).
- Freiwald, A., Fossa, J. H., Grehan, A., Koslow, T. & Roberts, J. *Cold-water Coral Reefs: Out of Sight—No Longer Out of Mind* (UNEP-WCMC, 2004).
- Honjo, S., Francois, R., Manganini, S. J., Dymond, J. R. & Collier, R. W. Particle flux in the Pacific sector of the Southern Ocean. PANGAEA <https://doi.org/10.1594/PANGAEA.787552> (2000).
- Honjo, S. Particle export and the biological pump in the Southern Ocean. *Antarct. Sci.* **16**, 501–516 (2004).
- Dadon, J. R. & de Cidre, L. L. The reproductive cycle of the thecosomatous pteropod *limacina retroversa* in the western South Atlantic. *Marine Biol.* **114**, 439–442 (1992).
- Franco, A. C., Gruber, N., Frölicher, T. L. & Kropuenske Artman, L. Contrasting impact of future CO₂ emission scenarios on the extent of the CaCO₃ mineral undersaturation in the Humboldt current system. *J. Geophys. Res. Oceans* **123**, 2018–2036 (2018).
- Lovenduski, N. S., Long, M. C. & Lindsay, K. Natural variability in the surface ocean carbonate ion concentration. *Biogeosciences* **12**, 6321–6335 (2015).
- Williams, N. L. et al. Assessment of the carbonate chemistry seasonal cycles in the Southern Ocean from persistent observational platforms. *J. Geophys. Res. Oceans* **123**, 4833–4852 (2018).

Acknowledgements

N.S.L., G.N.-G. and K.M.K. are grateful for support from the National Science Foundation (grant nos. OCE-1558225 and PLR-1543457). G.N.-G. was supported, in part, by the Significant Opportunities in Atmospheric Research and Science (SOARS) programme, NSF grant no. AGS-1641177. C.H. acknowledges support from the National Science Foundation (grant no. OCE-1459834). CESM computing resources were provided by CISL at NCAR. We thank B. Medeiros for providing model re-gridding scripts and N. Freeman for helpful comments on an earlier version of the manuscript.

Author contributions

N.S.L. and K.M.K. re-gridded the CESM-LE and CESM-ME DIC output to the GLODAP/WOA grid, corrected the model DIC bias and calculated the aragonite saturation state from the bias-corrected model DIC projections. S.K.L. provided the modified GLODAPv2 mapped climatologies and expertise. G.N.-G. analysed the bias-corrected projections and wrote the manuscript. All authors were involved in the study design, discussed the results and helped write the manuscript.

Competing interests

The authors declare no competing interests.

Additional information

Supplementary information is available for this paper at <https://doi.org/10.1038/s41558-019-0418-8>.

Reprints and permissions information is available at www.nature.com/reprints.

Correspondence and requests for materials should be addressed to N.S.L.

Journal Peer Review Information: *Nature Climate Change* thanks Nancy Williams and other anonymous reviewer(s) for their contribution to the peer review of this work.

Publisher's note: Springer Nature remains neutral with regard to jurisdictional claims in published maps and institutional affiliations.

© The Author(s), under exclusive licence to Springer Nature Limited 2019

Methods

Hydrographic and carbon chemistry observations. We use global mapped climatologies of ocean biogeochemical and physical variables collected via hydrographic cruises to identify the present-day Southern Ocean aragonite saturation horizon. DIC and alkalinity are taken from an adaptation of the Global Ocean Data Analysis Product for Carbon, version 2 (GLODAPv2) mapped product²³ that excludes artificial data along the GLODAPv2 mapping boundary at 20°E and includes only data that were quality controlled (that is, no profiles with a maximum sampling depth shallower than 1500 m and no profiles without crossovers)¹⁹. DIC observations were normalized to the year 2002 before mapping, by removing the temporal trends in DIC and pH due to anthropogenic influence^{19,20}. We used mapped climatologies of temperature, salinity, silicate, and phosphate from the WOA 2009 (refs. 31–33). GLODAP and WOA mapped products are on 1°×1° grids with 33 standard depth surfaces but here we only used the values in locations where there are observations. We used Mocsy 1.0 (ref. 34), a Fortran 90 package that determines the ocean carbonate system, to compute the annual mean saturation state of aragonite at every location and depth in the Southern Ocean. Mocsy uses DIC, salinity, temperature, alkalinity, phosphate and silicate in combination with the Lee et al.³⁵ formulation for total boron, first and second dissociation constants of carbonic acid (K_1/K_2) from Lueker et al.³⁶ and the Dickson and Riley³⁷ formulation for the equilibrium constant for hydrogen fluoride (K_f) on the total scale to compute carbonate chemistry variables. The saturation horizon was defined at each location as the depth where Ω_{Ar} is nearest 1.

CESM ensembles. We project future changes of the aragonite saturation horizon in the Southern Ocean using annual mean DIC output from the CESM-LE (2006–2100, 32 ensemble members analysed)⁸ and CESM-ME (2006–2080, nine ensemble members analysed)¹⁶. CESM is a state-of-the-art coupled climate model run with atmosphere, ocean (nominal 1° horizontal resolution and 60 vertical levels), land and sea ice components³⁸. All CESM ensemble members are exposed to the same external forcing: historical forcing from 1920 to 2005 and either RCP8.5 (CESM-LE) or RCP4.5 (CESM-ME) from 2006 onward. CESM-LE (RCP8.5) simulations were carried out to 2100, while CESM-ME (RCP4.5) simulations were carried out to 2080. Each ensemble member has a unique climate trajectory because of small round-off level differences in their atmospheric initial conditions⁸. All the CESM ensemble members began with an 1850 control simulation with constant pre-industrial forcing. The ocean model physical state was initialized to observations, while the ocean biogeochemical fields were initialized to a state derived from a separate 600-year spin-up. While these spin-ups resulted in a quasi-equilibrium for ocean biogeochemistry, we found significant biases in modelled, present-day Southern Ocean DIC as compared to observations (Supplementary Fig. 1; see also Long et al.³⁹).

We therefore used the procedure outlined in Orr et al.¹ and Ciais et al.¹¹ to make bias-corrected projections of the Southern Ocean aragonite saturation horizon from the two CESM ensembles. For each ensemble member and each projection year, we interpolated the model output to the GLODAP grid and calculated the annual mean DIC anomaly relative to the model estimate in 2002. We propagate this bias correction to 2100 in each ensemble member by adding the simulated model perturbations of DIC, relative to 2002, to the GLODAPv2 DIC climatology, while holding alkalinity, nutrients, temperature and salinity constant. As for the observations (see above), we used Mocsy³⁴ to calculate the resulting Southern Ocean aragonite saturation state from the bias-corrected DIC model projections. Here too the alkalinity, temperature, salinity, silicate and phosphate were all held constant at their present-day climatological values.

For a given year and desired depth level, ensemble mean values of the simulated variables were computed by averaging across ensemble members. Areas that on an annual average are covered in sea ice were omitted from our analysis due to well-known biases in the present-day CESM sea ice distribution⁴⁰. We define

sea ice extent as the northern-most grid point where the simulated sea ice fraction either equals or exceeds 0.2.

Seasonal bias. Since the Southern Ocean, due to its remoteness and prohibitive wintertime weather, is almost exclusively sampled during austral summer (December–March), the ship-based biogeochemical observations in GLODAPv2 contain a seasonal bias and very few grid points have data from all seasons. Even when data are available from all seasons, they are often collected many years apart, and these inter-annual variations challenge our ability to identify true seasonal variability. Despite studies showing that seasonal variations of temperature, surface mixed layer depth, and spring blooms have a noticeable impact on Ω_{Ar} and Ω_{Ca} in some regions of the global oceans⁴¹, no attempt has been made to correct for this seasonal bias in the GLODAPv2 mapped climatologies. This is due both to limited data coverage and that such corrections would have to rely on relationships with ancillary variables and different temporal gap-filling methods²⁰. The seasonal measurement bias remains one of the largest sources of unquantified uncertainty for the Ω_{Ar} and Ω_{Ca} estimates in the GLODAPv2 mapped climatologies.

Reporting Summary. Further information on research design is available in the Nature Research Reporting Summary linked to this article.

Data availability

CESM ensemble output is available from the Earth System Grid (<http://www.cesm.ucar.edu/projects/community-projects/LENS/data-sets.html>). GLODAPv2 data can be accessed from the project webpage (<https://www.glodap.info/>). WOA data are provided by the National Oceanographic Data Center (https://www.nodc.noaa.gov/OC5/WOA09/pr_woa09.html).

References

- Locarnini, R. A. et al. *World Ocean Atlas 2009* Vol. 1 (ed. S. Levitus) (NOAA Atlas NESDIS 68, 2010).
- Antonov, J. I. et al. *World Ocean Atlas 2009* Vol. 2 (ed. S. Levitus) (NOAA Atlas NESDIS 69, 2010).
- Garcia, H. E. et al. *World Ocean Atlas 2009* Vol. 4 (ed. S. Levitus) (NOAA Atlas NESDIS 71, 2010).
- Orr, J. C. & Epitalon, J.-M. Improved routines to model the ocean carbonate system: mocsy 2.0. *Geosci. Model Dev.* **8**, 485–499 (2015).
- Lee, K. et al. The universal ratio of boron to chlorinity for the North Pacific and North Atlantic oceans. *Geochim. Cosmochim. Acta* **74**, 1801–1811 (2010).
- Lueker, T. J., Dickson, A. G. & Keeling, C. D. Ocean cCO₂ calculated from dissolved inorganic carbon, alkalinity, and equations for k_1 and k_2 : validation based on laboratory measurements of CO₂ in gas and seawater at equilibrium. *Marine Chem.* **70**, 105–119 (2000).
- Dickson, A. G. & Riley, J. P. The estimation of acid dissociation constants in seawater media from potentiometric titrations with strong base. I. The ionic product of water – k_w . *Marine Chem.* **7**, 89–99 (1979).
- Hurrell, J. W. et al. The Community Earth System Model: A framework for collaborative research. *Bull. Am. Meteorol. Soc.* **94**, 1339–1360 (2013).
- Long, M. C., Lindsay, K., Peacock, S., Moore, J. K. & Doney, S. C. Twentieth-century oceanic carbon uptake and storage in CESM1(BGC). *J. Clim.* **26**, 6775–6800 (2013).
- Landrum, L., Holland, M. M., Schneider, D. P. & Hunke, E. Antarctic sea ice climatology, variability, and late twentieth-century change in CCSM4. *J. Clim.* **25**, 4817–4838 (2012).
- Jiang, L.-Q. et al. Climatological distribution of aragonite saturation state in the global oceans. *Global Biogeochem. Cycles* **29**, 1656–1673 (2015).

Reporting Summary

Nature Research wishes to improve the reproducibility of the work that we publish. This form provides structure for consistency and transparency in reporting. For further information on Nature Research policies, see [Authors & Referees](#) and the [Editorial Policy Checklist](#).

Statistical parameters

When statistical analyses are reported, confirm that the following items are present in the relevant location (e.g. figure legend, table legend, main text, or Methods section).

n/a | Confirmed

- The exact sample size (n) for each experimental group/condition, given as a discrete number and unit of measurement
- An indication of whether measurements were taken from distinct samples or whether the same sample was measured repeatedly
- The statistical test(s) used AND whether they are one- or two-sided
Only common tests should be described solely by name; describe more complex techniques in the Methods section.
- A description of all covariates tested
- A description of any assumptions or corrections, such as tests of normality and adjustment for multiple comparisons
- A full description of the statistics including central tendency (e.g. means) or other basic estimates (e.g. regression coefficient) AND variation (e.g. standard deviation) or associated estimates of uncertainty (e.g. confidence intervals)
- For null hypothesis testing, the test statistic (e.g. F , t , r) with confidence intervals, effect sizes, degrees of freedom and P value noted
Give P values as exact values whenever suitable.
- For Bayesian analysis, information on the choice of priors and Markov chain Monte Carlo settings
- For hierarchical and complex designs, identification of the appropriate level for tests and full reporting of outcomes
- Estimates of effect sizes (e.g. Cohen's d , Pearson's r), indicating how they were calculated
- Clearly defined error bars
State explicitly what error bars represent (e.g. SD, SE, CI)

Our web collection on [statistics for biologists](#) may be useful.

Software and code

Policy information about [availability of computer code](#)

Data collection

Provide a description of all commercial, open source and custom code used to collect the data in this study, specifying the version used OR state that no software was used.

Data analysis

Matlab

For manuscripts utilizing custom algorithms or software that are central to the research but not yet described in published literature, software must be made available to editors/reviewers upon request. We strongly encourage code deposition in a community repository (e.g. GitHub). See the Nature Research [guidelines for submitting code & software](#) for further information.

Data

Policy information about [availability of data](#)

All manuscripts must include a [data availability statement](#). This statement should provide the following information, where applicable:

- Accession codes, unique identifiers, or web links for publicly available datasets
- A list of figures that have associated raw data
- A description of any restrictions on data availability

CESM ensemble output is available from the Earth System Grid (<http://www.cesm.ucar.edu/projects/community-projects/LENS/data-sets.html>). GLODAPv2 data

Field-specific reporting

Please select the best fit for your research. If you are not sure, read the appropriate sections before making your selection.

Life sciences Behavioural & social sciences Ecological, evolutionary & environmental sciences

For a reference copy of the document with all sections, see [nature.com/authors/policies/ReportingSummary-flat.pdf](https://www.nature.com/authors/policies/ReportingSummary-flat.pdf)

Ecological, evolutionary & environmental sciences study design

All studies must disclose on these points even when the disclosure is negative.

Study description	Here, we quantify the depth of the present-day Southern Ocean aragonite saturation horizon using hydrographic and ocean carbon chemistry observations, and use a large ensemble of simulations from a single Earth System Model to track its evolution.
Research sample	We make use of output from a novel ensemble of simulations using a single Earth System Model. These model output have been made available via the Earth System Grid.
Sampling strategy	We evaluated a total of 32 ensemble members (the maximum available in the model archive).
Data collection	Model output were generated at the National Center for Atmospheric Research and made available via the Earth System Grid.
Timing and spatial scale	We analyzed simulations spanning 2005-2100.
Data exclusions	No data were excluded.
Reproducibility	Our analysis methods on the model output are completely reproducible.
Randomization	Each ensemble member was generated using a random, round-off level atmospheric temperature difference in 1920. Each ensemble member developed chaotically after this point.
Blinding	Each ensemble member was treated as an independent possible outcome.
Did the study involve field work?	<input type="checkbox"/> Yes <input checked="" type="checkbox"/> No

Reporting for specific materials, systems and methods

Materials & experimental systems

n/a	Involvement in the study
<input checked="" type="checkbox"/>	<input type="checkbox"/> Unique biological materials
<input checked="" type="checkbox"/>	<input type="checkbox"/> Antibodies
<input checked="" type="checkbox"/>	<input type="checkbox"/> Eukaryotic cell lines
<input checked="" type="checkbox"/>	<input type="checkbox"/> Palaeontology
<input checked="" type="checkbox"/>	<input type="checkbox"/> Animals and other organisms
<input checked="" type="checkbox"/>	<input type="checkbox"/> Human research participants

Methods

n/a	Involvement in the study
<input checked="" type="checkbox"/>	<input type="checkbox"/> ChIP-seq
<input checked="" type="checkbox"/>	<input type="checkbox"/> Flow cytometry
<input checked="" type="checkbox"/>	<input type="checkbox"/> MRI-based neuroimaging